Fabrication of S-shaped Micron Sized Constrictions on FeC (Steel) surface Using Femtosecond Laser Ablation with Beam Shaping

Patrice Umenne
Department of Electrical Engineering
University of South Africa
Johannesburg, South Africa
umennpo@unisa.ac.za

***Abstract*—In this paper we demonstrate the fabrication of S-shaped micron sized constrictions on steel surface using the femtosecond laser ablation technique. The femtosecond laser used has a wavelength of 775 nm, a power range of 0-1000 mW, a pulse duration of 130 fs and a pulse repetition rate of 1-2 kHz. The ultra-low pulse duration of 130 fs enables ablation of material surfaces without excessive thermal heating of the material around the zone of ablation. This becomes useful when ablating materials that are thermally sensitive such as superconducting thin films. This practice run of ablating S-shaped micron sized constrictions on steel surfaces shown in this paper will enable one to use the same technique in ablating micron and nano sized structures on superconducting thin films without thermally altering the superconductive film. In this paper S-shaped micron sized constrictions on steel were fabricated with a constriction width of 37.1 and 47.3 µm whose images were created using an optical microscope (OM) and S-shaped micron sized constrictions with a constriction width of 30.8 and 35.2 µm whose images were created using an atomic force microscope (AFM). The reduction in the constriction widths was achieved by reducing the laser ablation width or laser ablation spot size and then bringing the laser ablation spots closer together in G-code program. The reduction of the laser ablation width is achieved by reducing the laser fluence applied closer to the ablation threshold of steel and by using laser beam shaping techniques such as beam collimation and beam focusing.**

***Keywords*—Atomic Force Microscope (AFM), Beam Collimation, Femtosecond laser, Optical Microscope (OM), S-shaped Micron sized constrictions, Steel.**

I. INTRODUCTION

The main aim of this paper is to fabricate S-shaped micron sized constrictions on a steel surface using the femtosecond laser ablation technique. The fabrication of S-shaped micron sized constrictions on steel surface using the femtosecond laser was done as a trial run for the technique such that at a later stage the same technique for ablation can be used on superconducting thin films such as YBCO in the fabrication of superconducting bridges and Josephson junctions. The reason for using the femtosecond laser is because the femtosecond laser has a low pulse duration of 130 fs and as a result it was assumed it will not change the phase of a thermally sensitive material like a superconducting thin film around the zone of ablation. Around the zone of ablation, the superconductive thin film, should not experience much heating and change from a superconductive material to a normal one. The femtosecond laser used has a wavelength of 775 nm, a power range of 0-1000 mW, pulse duration of 130 fs and a pulse repetition or frequency of 1-2 kHz. The effect of the low-pulse duration of a femtosecond laser is evident in (1)[1],

$$E = P_{peak} * \tau \quad (1)$$

where E is the energy of the femtosecond laser, P_{peak} is the peak power emitted by the laser and τ is the pulse duration of the laser. Therefore, if the average power of the laser is set to 1000 mW, the pulse repetition rate is 1 kHz, the energy per pulse will be 1mJ. Then with a low pulse duration of 130 fs using (1), the peak power eminent from the femtosecond laser will be 7.7 GW.

The thermal heating of the material can be reduced by reducing the pulse energy of the laser. Reducing the pulse energy of the laser also reduces the laser ablation width or spot size of the laser. The pulse energy of the laser can be reduced by reducing the average power to 100 mW when ablating steel surfaces and increasing the pulse repetition rate or frequency of the laser to 2 kHz as in (2)[1],

$$P_{AVG} = E_{pulse} * Pulse_{rep.rate}(freq) \quad (2)$$

where P_{AVG} is the average power of the laser, E_{pulse} is the energy per pulse of the laser and $Pulse_{rep.rate}(freq)$ is the frequency or the pulse repetition rate of the laser. Such settings will generate an energy of 50 µJ. When carrying out micro structuring of a material in the low energy regime the ablation process leads to the formation of bubbles, which is a slight ablation. At higher pulse energies a molten ring forms around the holes and small droplets are observed as can be seen in Fig.1. This means that as the energy of the laser increases the size of the hole ablated also increases [2].

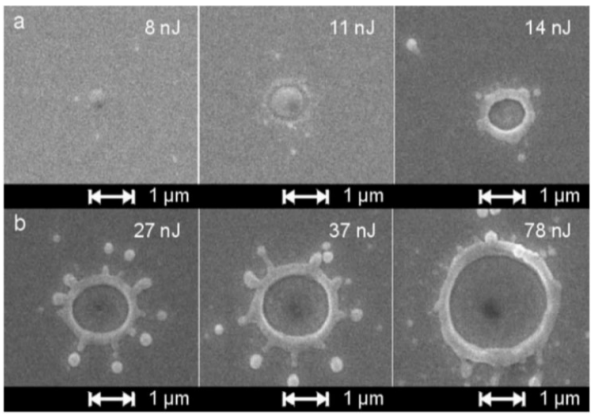

Fig. 1 Pulse Energy of the femtosecond laser vs. ablation holes diameters on chromium [2].

The same technique of ablating in the low energy regime to cut small laser ablation widths can be used in the fabrication of nano Josephson junctions.

II. METHODOLOGY

The S-shaped micron sized constriction fabricated on the steel surface in this paper is called an S-shaped constriction because just as the name implies it is shaped like the letter "S". The advantage of the S-shaped constriction structure is that it is possible to easily control the size of both the width and length of the constriction during the fabrication of the structure. The S-shaped structure is fabricated by using the G-code programming language to control the movement of a translation stage which holds the steel sample. The process of fabrication is as follows. Initially the laser beam is moved vertically up and down 5 mm along the length of the steel square sample as can be seen in Fig.2. This is done in order to ablate the ablation strip lines. The ablation strip lines are used to separate one constriction from another. The horizontal spacing between the vertical movements is about 5 µm wide and the complete ablation strip line covers about 0.5 mm width. Subsequently the laser beam is moved vertically down the length of the sample, the length of the movement is controlled by a short factor. Then the laser is moved horizontally into the sample and back out again. The laser is then moved vertically down along the length of the sample controlled by a long factor, across the width of the square sample by 1 mm. Vertically up to a specific position along the length controlled by a short factor, horizontally into the sample, back out again and then to the top of the square steel sample controlled by a long factor and begins the ablation strip lines again. A block diagram summarizing the S-shaped structure achieved can be seen in Fig.2.

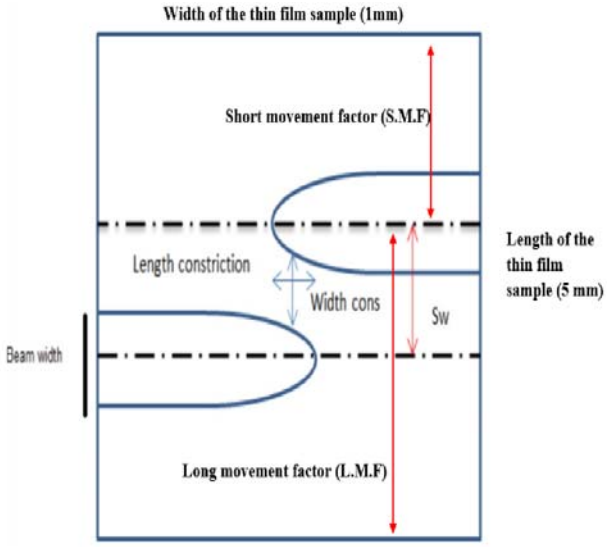

Fig. 2 S-shaped constriction fabrication [3,4]

In summary the width of the constriction fabricated on the steel surface is determined by (3),

$$width\ of\ the\ contriction\ on\ steel = S_w - Beam\ width \quad (3)$$

where S_W, is the separation distance between the centers of the laser ablation spots along the length of the steel sample and the *Beam width* is the laser ablation width.

A. Ablation Threshold

The ablation threshold of a material can be defined as the minimum amount of energy or power required to just start removing some of the surface material, in this case of the steel sample with the laser. The gaussian profile distribution of a laser relative to the ablation threshold of a material can be seen in Fig.3 below. The peak of the gaussian profile distribution depends on the laser power released from the source or the energy of the laser released. The cumulative energy of the laser will be equal to the total area of the gaussian profile distribution under the area of the curve. In order to ablate micron and sub-micron structures we need to reduce the laser ablation width of the laser to a minimum size. This can be achieved by using a laser fluence level which is slightly above the ablation threshold of the material with respect to the laser [2] as can be seen in Fig.3.

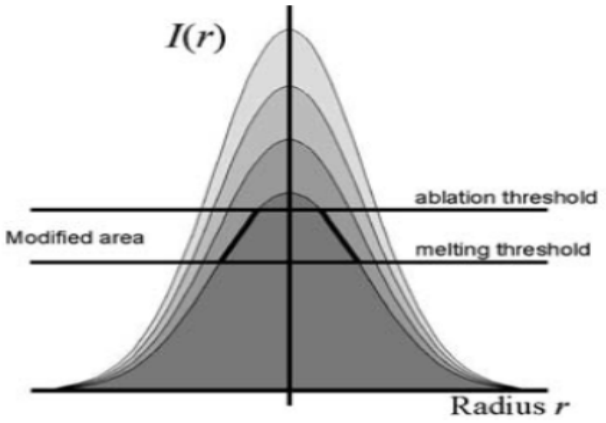

Fig. 3 Gaussian profile of a laser relative to the ablation threshold of a material [2]

It is possible to cut small structures by working slightly above the ablation threshold. This is achieved by varying the power of the laser eminent from the laser in the range 0-1000 mW. When ablating steel, the laser power is kept in the range 100-500 mW. This range is from low to medium above the ablation threshold of steel. The power eminent from the laser is measured by a power meter before the laser is focused unto the steel sample. Since we work slightly above the ablation threshold of the material only the central part of the laser beam ablates the sample which means we can reduce the laser ablation spot size and overcome the diffraction limit of the laser as stated in [2]. Equation (4) summarizes this principle,

$$F = F_0 \exp\left(-\frac{d^2}{d_0^2}\right) \quad (4)[2]$$

where d_0 is the laser ablation width, F_0 the peak laser fluence and F is the laser fluence applied to the steel surface. Using (4), the larger the laser fluence emitted from the laser, the larger the laser ablation width d_0 ablated on the steel surface. This effect is also detailed in [5].

B. Translation Stage and focusing optics

The translation stage consists of a platform with a mechanical part that is compressed with argon gas. The translation stage moves the platform in 3 dimensions (x, y, z). The platform holds the steel sample that is ablated to fabricate the S-shaped constriction on steel. The test run of the S-shaped design on steel surfaces can be used to fabricate similar S-shaped nano Josephson junctions [6] using the femtosecond laser. The S-shaped structure makes it possible to control the width and length of the constriction during fabrication. The translation stage can be seen in Fig. 4 below.

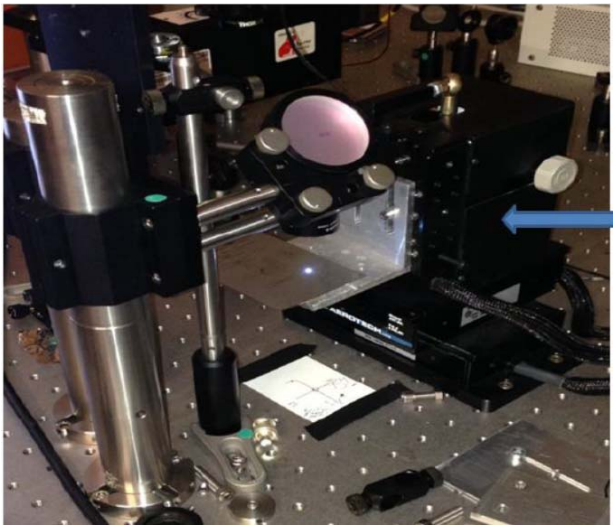

Fig. 4 Translation stage

The translation stage operates with a reflective mirror held in position above the focusing lens or optics. The focusing lens focuses the beam unto the steel sample and the pattern is machined on the sample. The x-y axis can be seen below the platform. The focusing lens used was either a conventional spherical convex lens of focal length 30, 45 mm or an objective plano convex lens of numerical aperture NA 0.25. The objective lens focuses the laser beam more than the conventional spherical lenses and can produce a much smaller laser ablation width.

C. Beam Collimation and Beam Shaping

Beam collimation involves spreading out or expanding a beam and then making the beam parallel. A perfectly collimated beam would not disperse with distance. The laser beam is collimated and then focused using the focusing lenses described in section II.B. There are two reasons for collimating the laser beam in this project. The first reason is because the laser beam emanating from the laser source was elliptical not spherical in shape, with the x-axis slightly smaller than the y-axis as a result there was a need to expand the x-axis. The second reason is that by expanding the laser spot before focusing with the focusing optics it will be possible to produce a smaller laser ablation spot for the fabrication of micron/submicron structures on surfaces. The laser beam can be expanded by using a cylindrical diverging lens and then collimated with a cylindrical converging lens as can be seen in Fig. 5. Geometrically cylindrical lenses are half the sphere in a spherical lens.

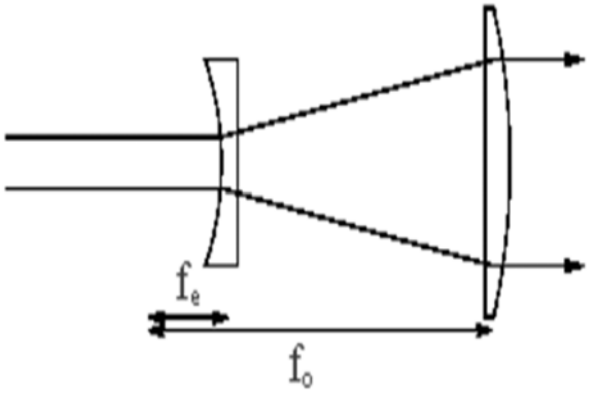

Fig. 5 Cylindrical lenses collimating a beam

In this paper a cylindrical diverging lens of -50 mm focal length and a cylindrical converging lens of +100 mm with an aperture diameter of $25 \times 25\,mm$ were used. When cylindrical lenses are used you can spread out the axis that is aligned perpendicularly to the normal axis of the lenses. Since in this case we wanted to expand the x-axis of the laser beam, we kept the y-axis of the beam aligned to the normal axis of the lenses and the x-axis of the beam perpendicular to the normal axis of the lenses. The laser beam can only collimate when the lenses are separated by a specific distance along the beam path. When the ratio of the focal length between the cylindrical converging lens in this case +100 mm and the cylindrical diverging lens in this case -50 mm is equal to a factor of 2, then the separation distance between the two lenses from their centers will be equal to the focal length of the cylindrical diverging lens in this case 50 mm. The actual set up of the cylindrical lenses for beam collimation can be seen in Fig.6.

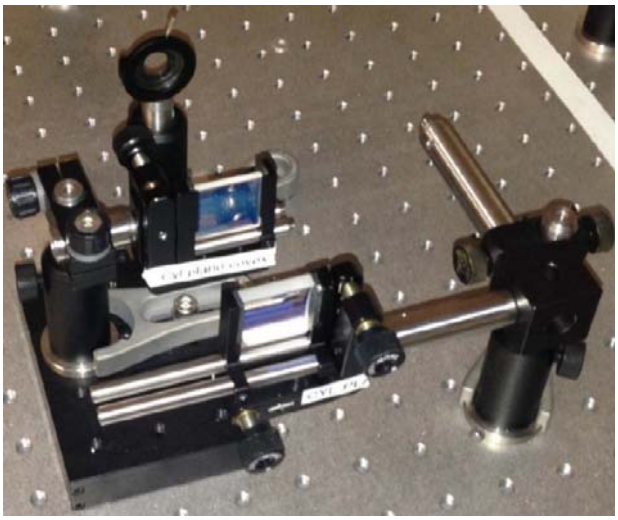

Fig. 6 3-D view of the Cylindrical lenses during beam collimation

The iris diaphragm in Fig. 6 is set to an aperture diameter of 1.5 mm in order to allow only the central core of the laser beam to pass through and to remove any unwanted peripheral components of the beam. This also helps to further reduce the laser ablation spot size.

III. Results

When using the femtosecond laser to fabricate S-shaped constrictions on steel, the laser starts to cut at a power level of approximately 50 mW, indicating the ablation threshold of steel with respect to the laser is approximately 50 mW. Constrictions were fabricated on steel between a power range of 100-500 mW. A constriction of width 37.1 µm at a power setting of 483 mW and a constriction of width 47.3 µm at a power setting of 224 mW were fabricated using the femtosecond laser. The images of these S-shaped constrictions were created using an optical microscope (OM). A constriction of width 30.8 µm at a power setting of 220 mW and a constriction of width 35.2 µm at a power setting of 104 mW were also fabricated. The images of the latter S-shaped constrictions were created using the atomic force microscope (AFM). Table I summarizes the laser settings used to fabricate the S-shaped constrictions on steel.

TABLE I LASER SETTINGS FOR THE FABRICATION OF THE S-SHAPED CONSTRICTIONS ON STEEL AND THEIR DIMENSIONS

Name of S-shaped constriction	Laser Power (mW)	Width of the constriction (µm)	Separation distance between the centers of laser ablation spots along the length of sample (S_W)	Beam width or laser ablation width (µm)	Tool used for imaging of constriction
Micron-steel I	483 mW	37.1 µm	82 µm	40 µm	Optical Microscope (OM)
Micron-steel II	224 mW	47.3 µm	82 µm	30.7 µm	Optical Microscope (OM)
Micron-steel III	220 mW	30.8 µm	60 µm	30.4 µm	Atomic Force Microscope (AFM)

Micron-steel IV	104 mW	35.2 µm	60 µm	25.7 µm	Atomic Force Microscope (AFM)

Table I shows that as the laser power level decreases the laser ablation width also decreases. This validates the theory that as the laser fluence is reduced the laser ablation width reduces. This theory can be used to fabricate micron and sub-micron structures.

A. Micron-steel I at power 483 mW

At a laser power setting of 483 mW the laser ablation width produced on the steel surface is 40 µm. The separation distance between the centers of the laser ablation spot along the length of the sample (S_W) in the G-code program is 82 µm. The Micron-steel I constriction fabricated on steel has a width of 37.1 µm. These laser settings combined with the achieved width of the constriction validate the derived formula given in (3). That is the $width\ of\ the\ contriction\ on\ steel = S_w - Beam\ width$. The average percentage error in using the method to fabricate S-shaped constrictions on steel of a specific width is approximately ±7%. This percentage error can be reduced by repetition of the technique and by using the AFM to take measurements since its more precise. Figure 7 shows the image of the Micron-steel I constriction fabricated on steel with a width of 37.1 µm. The image is taken using an optical microscope (OM).

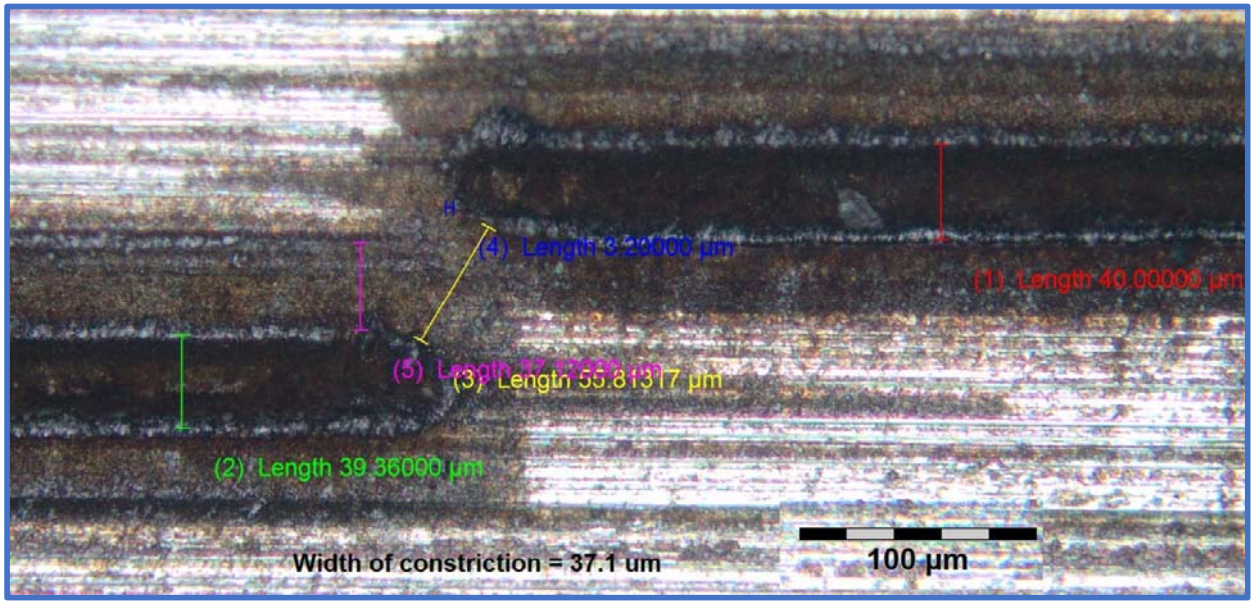

Fig. 7 Micron-steel I constriction width of 37.1 µm at power of 483 mW

B. Micron-steel II at power 224 mW

When the laser power setting is 224 mW the laser ablation width achieved is 30.7 µm. The separation distance between the centers of the laser ablation spot along the length of the sample (S_W) set in the G-code program is still 82 µm. The Micron-steel II constriction has a width of 47.3 µm. Figure 8 shows the image of the Micron-steel II constriction with a width of 47.3 µm. The image shows that there is a central core of ablation and secondary fringe of ablation. This indicates that there is an element of heating within the width of the constriction from the laser. This secondary fringe of heating can be eliminated by reducing the diameter of the iris aperture used before the focusing optics. The image also shows that there is some steel debris around the central core. This occurs as a result of the rapid cooling of steel immediately after ablation.

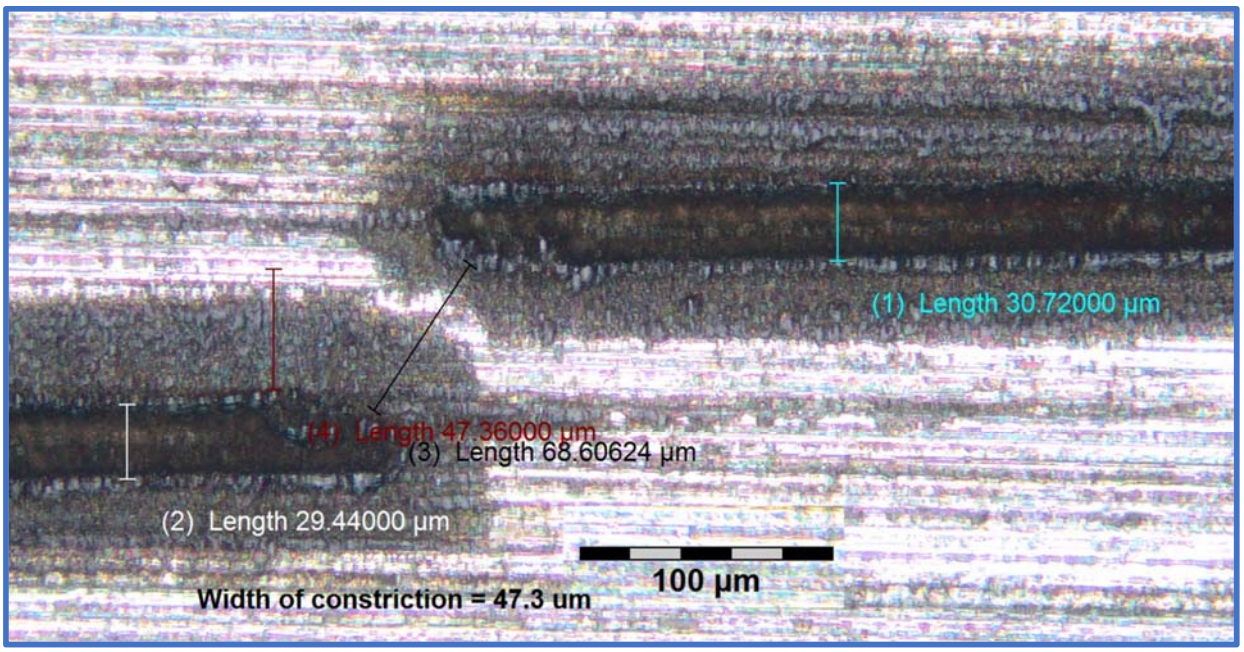

Fig. 8 Micron-steel II constriction of width 47.3 µm at power of 224 mW

C. Micron-steel III at power 220 mW

In the case of the Micron-steel III constriction the power is set to 220 mW and the laser ablation width achieved is 30.4 µm. The separation distance between the centers of the laser ablation spot along the length of the sample (S_W) set in the G-code program is now reduced to 60 µm. As a result, the width of the Micron-steel III constriction reduces to 30.8 µm. In this constriction the image is taken using an atomic force microscope (AFM). The resultant image of the constriction can be seen in Fig. 9a. and Fig. 9b.

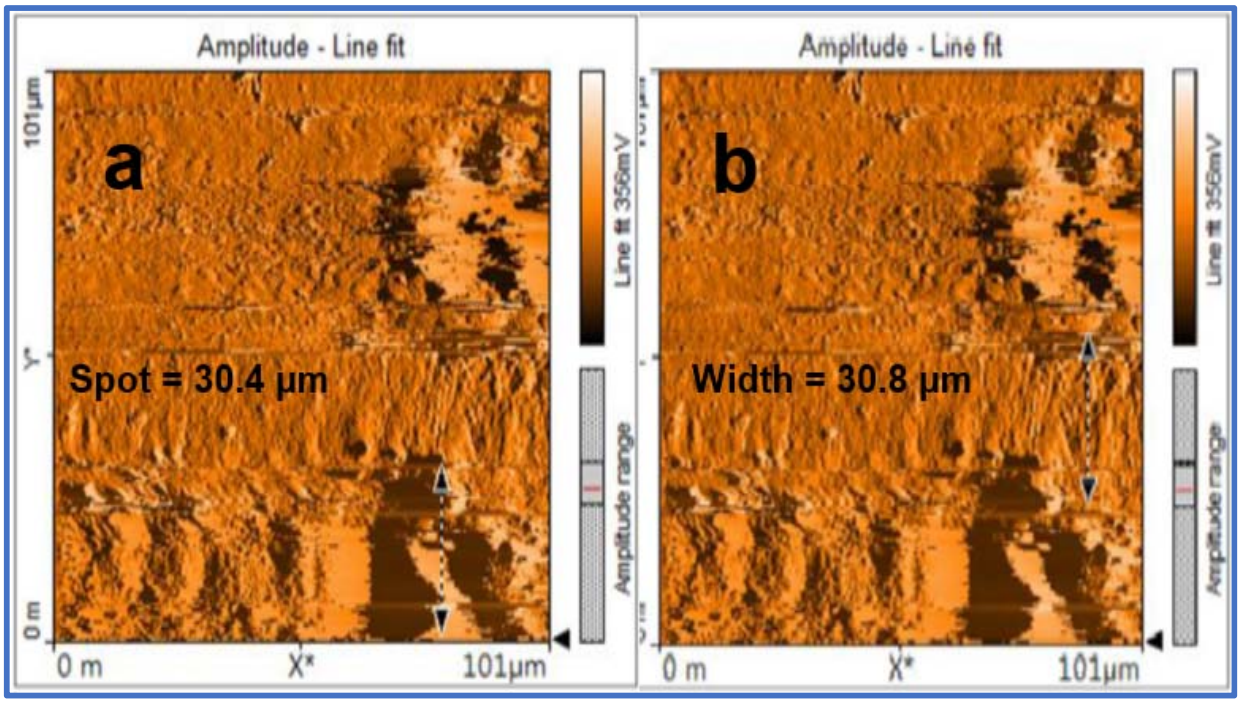

Fig. 9a. Micron-steel III Laser ablation spot size and **Fig.9b**. Micron-steel III constriction width

D. *Micron-steel IV at power 104 mW*

In the case of the Micron-steel IV constriction the power is set to 104 mW and the laser ablation width is 25.7 µm. The separation distance between the centers of the laser ablation spot along the length of the sample (S_W) set in the G-code program is kept at 60 µm. The width of the Micron-steel IV constriction becomes 35.2 µm. The image for this constriction is created using an atomic force microscope (AFM). The image for the constriction can be seen in Fig. 10a. and Fig. 10b.

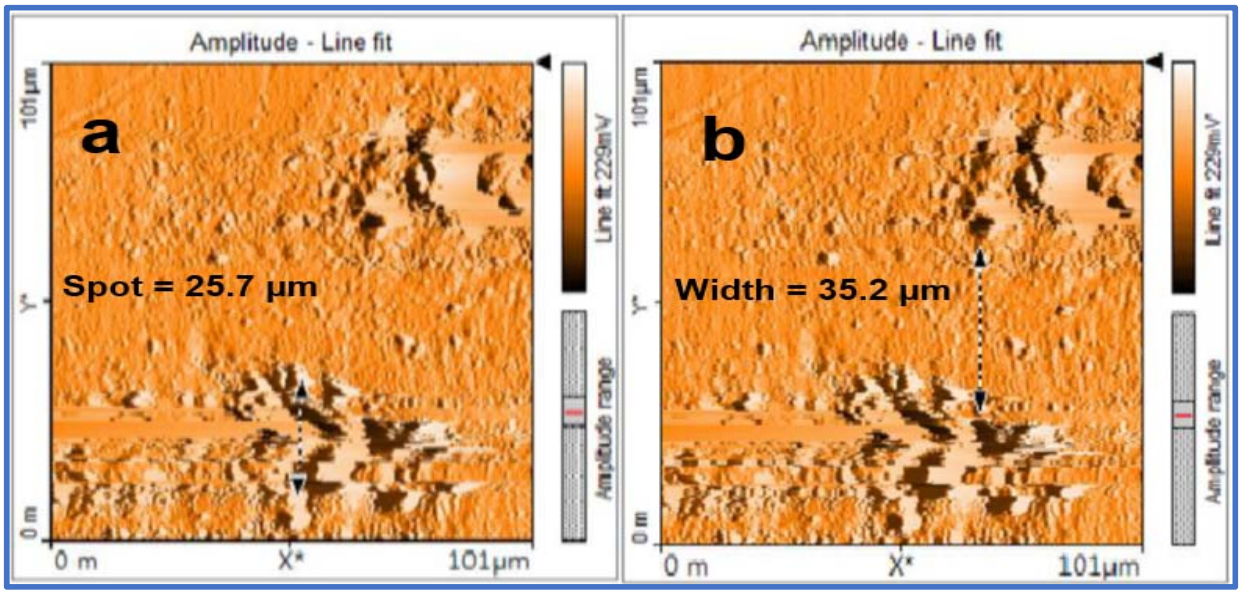

Fig. 10a. Micron-steel IV Laser ablation spot size and **Fig. 10b.** Micron-steel IV constriction width

IV. Conclusion

In conclusion the femtosecond laser was used to fabricate S-shaped micron sized constrictions on steel with a constriction width of 37.1 µm (Micron-steel I) and constriction width of 47.3 µm (Micron-steel II). The images of these were created using an optical microscope (OM). S-shaped micron sized constrictions with a constriction width of 30.8 µm (Micron-steel III) and constriction width of 35.2 µm (Micron-steel IV) were also fabricated and viewed using an atomic force microscope (AFM). Beam collimation was used as a beam shaping technique to facilitate the reduction of the laser ablation spot size which will assist in the micro structuring of materials. The theory that reducing the laser fluence will reduce the laser ablation width [2] was validated in experiments. The width of the constriction was determined to be equal to $S_w - Beam\ width$. The average percentage error of using this method to fabricate S-shaped constrictions of a specific width is approximately ±7%. The percentage error could be improved by repetition of the technique and by using an AFM to take the measurements for precision. There is a marginal amount of thermal heating from the femtosecond laser around the periphery of the laser ablation width. This femtosecond laser technique can be used to fabricate nano Josephson junctions [7-10].

Acknowledgment

I would like to acknowledge the resources and support provided by the University of South Africa in the completion of this project.

DECLARATION

Ethical Approval
Not Applicable

Consent to participate
Not Applicable, no humans or animals where involved in this study.

Consent to publish
I am the sole author in this publication and give consent to publish.

Author Contribution
I am the sole author in this work and have done the work and experiments, required to collect the data to write the paper.

Funding
All resources used to generate the data to produce this manuscript where provided by the University of South Africa (UNISA) which whose affiliation is acknowledged in the work.

Competing Interests
Not Applicable, there are no competing interests.

Availability of Data and Materials
Not applicable.

REFERENCES

[1] COHERENT, Measuring Laser Power and Energy Output, Available Online: http://www.coherent.com/

[2] F. Korte *et al.*, Towards nanostructuring with femtsecond laser pulses, *Applied Physics A*, vol. 77, pp 229-235, 2003, Available online: doi: 10.1007/s00339-003-2110-z.

[3] P. Umenne, Fabrication of Nano Josephson Junctions Using the Femtosecond Laser Technique on high T_C Superconducting $YBa_2Cu_3O_7$ Thin Films, *PhD Thesis, University of South Africa*, 2017, Available Online: http://hdl.handle.net/10500/23646.

[4] P. Umenne and V.V Srinivasu, Femtosecond laser fabrication of micron and sub-micron sized S-shaped contrictions on high T_C superconducting $YBa_2Cu_3O_{7-x}$ thin films: ablation and lithography issues, J. Mater. Sci.: Mater. Electron., vol. 28, pp. 5817-5826, 2017, Available Online: doi: 10.1007/s10854-016-6253-z.

[5] A.I. Kuznetsov, J. Koch and B.N. Chichkov, Nanostructuring of thin gold films by femtosecond lasers, Appl. Phys. A, vol. 94, pp. 221-230, 2009, Available Online: doi: 10.1007/s00339-008-4859-6.

[6] A.A.O Elkaseh *et al.*, Nanoplough-Constrictions on Thin YBCO Films Made with Atomic Force Microscopy, *Journal of Nanoscience and Nanotechnology*, vol. 7, no. 9, pp. 3348-3349, 2007, Availble Online: doi: 10.1166/jnn.2007.892.

[7] U. Buttner, G.L. Hardie, R. Rossouw, V.V Srinivasu and W.J. Perold, Fabrication of submicron YBCO Josephson junctions by a sample mosaic navigation assisted laser etching process, Supercond. Sci. Technol., vol. 20, no. 11, pp. S426-S429, 2007, Available Online: doi: 10.1088/0953-2048/20/11/S24

[8] W.F. van staden *et al.*, A novel buffered high-T_C superconducting step-edge Josephson junction, *Supercondcutor Science and Technology*, vol. 20, no. 11, pp. S419-S425, 2007, Available Online: doi: 10.1088/0953-2048/20/11/S23.

[9] J. Du, T. Zhang, Y.J. Guo and X.W. Sun, A high-temperature superconducting monolithic microwave integrated Josephson down-converter with high conversion efficiency, Appl. Phys. Lett., vol. 102, pp. 212602, 2013, Available Online: doi: 10.1063/1.4808106.

[10] A.A.O. Elkaseh, V.V. Srinivasu and W.J. Perold, Observation of Shapiro-Steps in AFM-Plough Micron-Size YBCO Planar Constrictions, IEEE Trans. Appl. Supercond., vol. 19, no.3, pp. 187-190, 2009, Available Online: doi: 10.1109/TASC.2009.2018542.